were first observed and brought to our attention by Z. J. Kiss, and the initial quantitative investiga-

tions were made by P. Asbeck while he was a summer employee at RCA Laboratories.

[1]B. W. Faughnan, Phys. Rev. (to be published).

[2]K. A. Müller, Th. von Waldkirch, W. Berlinger, and B. W. Faughnan, Solid State Commun. 9, 1097 (1971).

[3]B. W. Faughnan and Z. J. Kiss, IEEE J. Quant. Electron. QE-5, 17 (1969).

[4]B. W. Faughnan and Z. J. Kiss, Phys. Rev. Letters 21, 1331 (1968).

[5]T. C. Ensign and S. E. Stokowski, Phys. Rev. B 1, 2799 (1970).

[6]K. A. Müller, W. Berlinger, and R. S. Rubin, Phys. Rev. 186, 361 (1969).

[7]See R. N. Tredgold, Space Charge Conduction in Solids· (Elsevier, Amsterdam, 1966).

[8]B. W. Faughnan and Z. J. Kiss (unpublished).

[9]M. S. Kosman and E. V. Bursian, Dokl. Akad. Nuak SSSR 115, 483 (1957) [Sov. Phys. Doklady 2, 354 (1957)].

[10]O. N. Tufte and P. W. Chapman, Phys. Rev. 155,

796 (1967).

[11]L. C. Walters and R. E. Grace, J. Phys. Chem. Solids 28, 239 (1967); 28, 245 (1967).

[12]See R. C. Bradt and G. S. Ansell, J. Am. Ceram. Soc. 52, 192 (1969), for a recent analysis with extensive bibliography.

[13]R. Williams, J. Phys. Chem. Solids 26, 399 (1965).

[14]E. M. Pell, J. Appl. Phys. 31, 291 (1960).

[15]D. L. Staebler and J. Blanc (unpublished).

[16]J. E. Carnes and A. M. Goodman, J. Appl. Phys. 38, 3091 (1967).

[17]M. A. Lampert and P. Mark, Current Injection in Solids (Academic, New York, 1970), p. 189.

[18]A. E. Paladino, J. Am. Ceram. Soc. 43, 476 (1965).

[19]A. E. Paladino, L. G. Rubin, and J. S. Waugh, J. Phys. Chem. Solids 26, 391 (1965).

Even-Parity Lattice Resonances and Anharmonicity in KI: Ag+

R. D. Kirby*†

Department of Physics and Materials Research Laboratory,‡ University of Illinois, Urbana, Illinois 61801 and Laboratory of Atomic and Solid State Physics,§Cornell University, Ithaca, New York 14850
(Received 6 July 1971)

We report here the observation of four impurity-induced lattice resonances in KI:Ag+. In addition to the well-known T_{1u} symmetry resonant mode at 17.3 cm^{-1}, we have observed two even-parity resonant modes of A_{1g} and E_g symmetries at 25 and 16.35 cm^{-1}, respectively, and a T_{1u} symmetry gap mode at 86.2 cm^{-1}. The two even-parity modes were detected using far-infrared spectroscopic techniques with the sample in an external electric field. The field induces a strong mixing of the modes of opposite parity and results in large field-induced shifts. The E_g symmetry resonance has also been seen in the Raman spectrum of KI:Ag+. Two weak and broad absorption lines at 29.8 and 44.4 cm^{-1} are attributed to the $E_g + T_{1u}$ and $A_{1g} + T_{1u}$ combination bands, respectively. These results are interpreted in terms of a model in which the T_{1u} symmetry resonant mode is anharmonically coupled to the even-parity resonances.

I. INTRODUCTION

In recent years there have been a variety of experimental and theoretical investigations of the vibrational properties of substitutional impurities in alkali halides. Thus far, most of the work has been concerned with an understanding of the odd-parity (optically active) local,[1-7] gap,[8,9] and resonant[10-15] modes. However, there can also be impurity-activated resonances with even parity. These modes do not involve any motion of the impurity ion itself, and because of their even parity, will not be optically active in the absence of an external perturbation. To date, even-parity modes have received little attention, apparently because of the difficulties

involved in detecting and identifying them.

Both even-parity resonant and gap modes have been observed indirectly as sidebands of the infrared-active U-center local mode in KI and KBr.[1-3] The sidebands were made optically active by an anharmonic coupling between the even-parity resonant and gap modes and the odd-parity local mode. In a lattice-dynamical calculation, Gethins et al.[16] found it necessary to include rather large force-constant changes between the impurity ion's nearest neighbors and its fourth nearest neighbors (along [100]) to obtain some quantitative agreement with the experimental results of Timusk and Klein.[3]

There is evidence that even-parity resonances have been observed in low-temperature thermal-

conductivity measurements on doped alkali halides. In KI : Ag$^+$,[17] KBr : Li$^+$,[18] and NaCl: Cu$^+$,[19] low-temperature dips in the thermal conductivity were observed which did not appear at the correct temperatures to be due to the well-known infrared-active resonances in these systems. However, thermal conductivity is basically a broad-band technique and cannot as of yet furnish precise information on the frequencies, linewidths, or symmetries of the observed resonances.

KI : Ag$^+$ is known to have a T_{1u} symmetry resonant mode at 17.3 cm^{-1}.[10,13] We report here the observation of two even-parity resonant modes of A_{1g} and E_g symmetries in KI:Ag$^+$ and offer evidence for an anharmonic coupling between resonances of opposite parity.

In Sec. II, the experimental results of far-infrared-absorption measurements and Raman-scattering measurements on Ag$^+$-doped KI are reported. These two experimental techniques allow the observation of both odd-parity and even-parity resonances.

In Sec. III, we develop a model in which the 17.3-cm^{-1} T_{1u} symmetry resonant mode in KI : Ag$^+$ is anharmonically coupled to the observed even-parity resonances of A_{1g} and E_g symmetries, and in Sec. IV, the predictions of this model are compared with the various experimental results.

In Sec. V of this paper, we speculate on the causes of some of the discrepancies between the model and experiment, and in the Appendix, we consider the effects of a second-order dipole moment on the experimental properties of KI : Ag$^+$.

A preliminary report of some of these results has been given elsewhere.[20]

II. EXPERIMENTAL TECHNIQUES AND RESULTS

A. Far-Infrared Transmission Measurements

The single-crystal pure and doped KI samples studied in this investigation were grown in an argon atmosphere using the Kyropolous technique. Samples were obtained both from the Crystal Growth Facility at Cornell University and from Dr. F. Rosenberger at the Crystal Growth Laboratory of the University of Utah. No differences were seen in the spectra of the samples obtained from the two sources.

The far-infrared transmission measurements on the pure and doped KI samples were made using interferometric spectrometers in conjunction with cooled germanium bolometers. Most of the impurity-induced absorption measurements were made with a modified RIIC FS 720 Michelson interferometer and a Ga-doped germanium bolometer detector operating at 1.2 K. The samples to be studied were mounted on a rotatable sample ring in a separate chamber of the detector cryostat, and were cooled to 4.2 K by exchange gas coupling to the outer helium bath.

The absorption spectra were obtained by measuring the far-infrared transmission through both the pure and doped KI samples. This technique yields the impurity-induced absorption coefficient.

All of the electric-field-dependence measurements were made with a lamellar interferometer[21] and a Ge bolometer cooled to 0.4 K.[22,23] The samples were immersed in liquid He at 4.2 K for these measurements. The experimental techniques involved in making these measurements have been described elsewhere.[24]

Figure 1 shows the KI : Ag$^+$ far-infrared absorption spectrum at 4.2 K with an instrumental resolution of 0.25 cm^{-1}. This particular sample contained 100-ppm Ag by weight. The spectrum is seen to be complicated, with at least seven Ag-induced absorption lines. The dominant features of the absorption spectrum are the well-known resonant mode at 17.3 cm^{-1} and the gap mode at 86.2 cm^{-1}. The resonant mode is slightly broadened by the presence of the two naturally occurring Ag isotopes (107 and 109 amu) in nearly equal amounts. The isotopic shift of the gap mode has not yet been measured, but is expected to be small.[9,25] The spectrum in the region of the gap mode was slightly distorted by two relatively weak absorption lines which were present in both pure and doped samples in unequal amounts. These two lines have the same frequencies (86.3 and 86.9 cm^{-1}) and relative intensities as two of the lines observed by Renk in OH$^-$-doped KI.[26] Becker[27] has shown that these lines are not due to OH$^-$ impurities. Furthermore, we found no evidence of the 69.7-cm^{-1} OH$^-$-induced line observed by him. In any case, these two lines are not due to Ag$^+$, and their effect ($\sim 10\%$) on the observed absorption spectrum has been roughly subtracted out. Thus, the solid curve in the gap-mode region of Fig. 1 shows our estimate of the real Ag$^+$-induced absorption line.
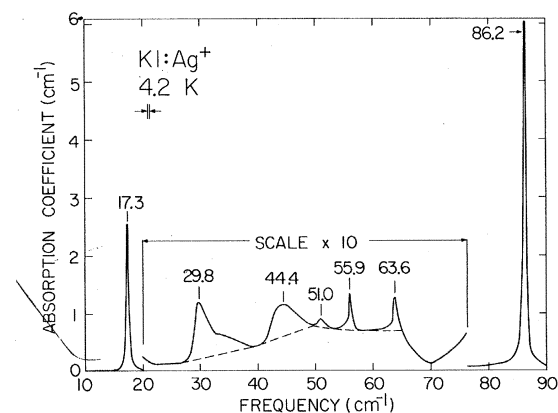

FIG. 1. Far-infrared absorption spectrum of KI:Ag$^+$ at 4.2 K. The instrumental resolution is 0.25 cm^{-1}.

TABLE I. Observed far-infrared absorption lines in KI:Ag$^+$.

Frequency (cm^{-1})	Linewidth (cm^{-1})	Absorption strength
17.3	0.60	1.0
29.8	3.2	0.3
44.4	6.6	0.2
51.0	1.6	0.01
55.9	0.5	0.05
63.6	0.9	0.04
86.2	0.65	4.0

An absorption peak also occurs at 29.8 cm^{-1}, with a broad shoulder at ~32.8 cm^{-1}. The 44.4-cm^{-1} line is similar to the 29.8-cm^{-1} line in width and strength. The three remaining lines at 51, 55.9, and 63.6 cm^{-1} are relatively much weaker and narrower.

The observed absorption spectrum varies linearly in absorption strength with Ag concentration, although the 51-cm^{-1} line is too weak to be observed at any but the highest concentrations. The whole absorption spectrum shows the same peculiar aging effect which was reported earlier for the resonant mode.[13] For example, in one sample, the absorption strength of the resonant mode decreased by a factor of 12 over a period of 15 months. No trace of the 78-cm^{-1} line which was reported to appear after heat treatment[13] was found in this particular sample. This indicates that more than one type of aging mechanism exists.

The observed KI:Ag$^+$ absorption frequencies, linewidths [full widths at half-maximum (FWHM) absorption], and integrated absorption strengths (areas under the absorption lines) are summarized in Table I. The absorption baselines chosen for the purpose of measuring the linewidths and strengths are indicated in Fig. 1. It should be noted that these baselines are somewhat arbitrary. No corrections for the finite spectrometer resolution have been made, but these corrections are expected to be small.[13]

B. Electric-Field Dependence of the Absorption Spectrum

Figure 2 shows the results of a typical KI:Ag$^+$ electric-field-dependence measurement. An external electric field (E_{dc}) of 175 kV/cm was applied in the [100] crystallographic direction, and the electric-field vector of the incident far-infrared radiation (E_{ir}) was polarized parallel to E_{dc}. These data were obtained by dividing the field-on transmission spectrum by the zero-field transmission spectrum and result in the "electric-field-induced absorption coefficient" ($\Delta\alpha$). In this case, a negative $\Delta\alpha$ indicates a decrease in absorption with applied field, while a positive $\Delta\alpha$ indicates a field-induced in-
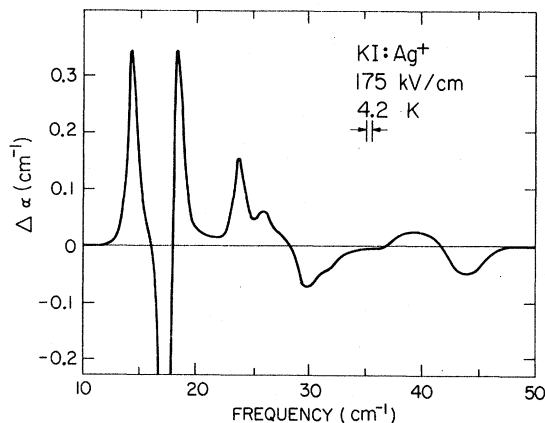

FIG. 2. Electric-field-induced absorption coefficient for KI:Ag$^+$. Here, $E_{ir} \| E_{dc} \|$ [100], and the instrumental resolution is 0.55 cm^{-1}.

crease in absorption at that particular frequency. Clearly, a shift in the absorption frequency of a line will give rise to a negative $\Delta\alpha$ near the unperturbed absorption frequency and a positive $\Delta\alpha$ near the perturbed line position. In the general case, both field-induced dichroisms and shifts are expected to occur.

In the high-field region, much of the field-shifted structure is almost completely resolved from the zero-field structure. In this limit, the zero-field absorption spectrum [$\alpha(0,\nu)$] can be obtained directly from the negative part of the $\Delta\alpha(E,\nu)$ curve. Then the impurity-induced absorption spectrum with applied field E can be obtained from the relation

$$\alpha(E,\nu) = \alpha(0,\nu) + \Delta\alpha(E,\nu) . \qquad (1)$$

The results of carrying out this procedure for a
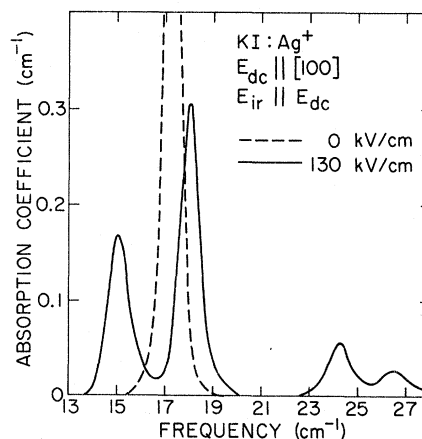

FIG. 3. KI:Ag$^+$ absorption spectrum below 20 cm^{-1} with a dc electric field of 130 kV/cm applied along [100]. Here, $E_{ir} \| E_{dc}$, and the instrumental resolution is 0.35 cm^{-1}.
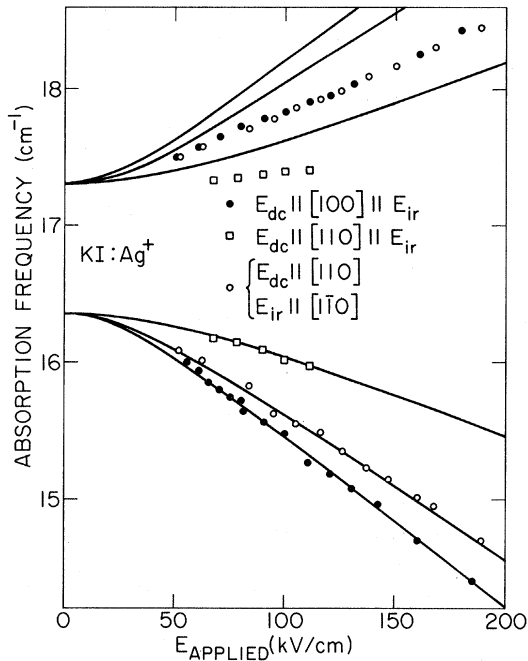
FIG. 4. Frequency vs external electric-field results for the T_{1u} and E_g symmetry resonances in KI:Ag$^+$. The solid curves were fitted using the anharmonic-oscillator model described in Sec. III.

typical measurement are shown in Fig. 3. Here, $E_{dc} \parallel [100] \parallel E_{ir}$. The solid curve shows the KI:Ag$^+$ resonant-mode absorption line in zero field. The dashed curve shows the observed absorption spectrum for $E_{dc} = 130$ kV/cm. The field dependence of this spectrum shows that the 18-cm^{-1} line is due to the field-shifted component of the (T_{1u} symmetry) resonant mode. It shifts up in frequency and decreases in strength with increasing field. The line near 15.5 cm^{-1} appears only when a field is applied. It shifts down in frequency and increases in strength with increasing field. The behavior of these two lines is characteristic of two modes of opposite parity being mixed by the (odd-parity) electric field. It will be shown that this is indeed the case and that the lower frequency mode has E_g symmetry in zero field.

A somewhat similar field dependence is seen in the 24–30-cm^{-1} region of Fig. 2. One component of the 29.8-cm^{-1} line shifts to lower frequencies and decreases in strength with increasing field. Simultaneously, the 25-cm^{-1} line grows in strength and also shifts down in frequency. We shall show that the 25-cm^{-1} line has A_{1g} symmetry in zero field. However, the mixing in this case is complicated because both lines shift down in frequency. This will be discussed in more detail in Sec. IV.

[100]-field measurements have been made for $E_{ir} \parallel E_{dc}$ and $E_{ir} \perp E_{dc}$. For a [110] electric field,

there are three distinct polarization directions corresponding to $E_{ir} \parallel E_{dc}$, $E_{ir} \parallel [1\bar{1}0] \perp E_{dc}$, and $E_{ir} \parallel [001] \perp E_{dc}$. Field-dependence measurements have been made for all three polarization directions. The field-induced shifts for the two lines in the 17-cm^{-1} region are summarized in Fig. 4. For those polarization directions not shown, no shifts were observed. The frequency shifts in all cases are found to be linear with field in the high-field limit. The frequency-vs-field curves for the lower frequency line could not be extended into the low-frequency region because of its vanishing absorption strength and its proximity to the resonant-mode absorption line. For these reasons the zero-field frequency of this line is known only to an accuracy of 16.35 ± 0.1 cm^{-1}. The meanings of the solid curves in Fig. 4 will be explained in Sec. IV.

For a [100] field, frequency shifts are observed only for $E_{ir} \parallel E_{dc}$. For a [110] field, no shifts are found with $E_{ir} \parallel [001]$. We now use these results to show that the 16.35-cm^{-1} mode does have E_g symmetry. With a [100] external field, the defect site symmetry is reduced from O_h to C_{4v}, so that an E_g mode splits into two levels, transforming as the A_1 and B_1 irreducible representations of C_{4v}. Of these, only the A_1 is optically active, and then only for $E_{ir} \parallel E_{dc}$. For a [110] applied field, the site symmetry becomes C_{2v} and the E_g mode splits into levels
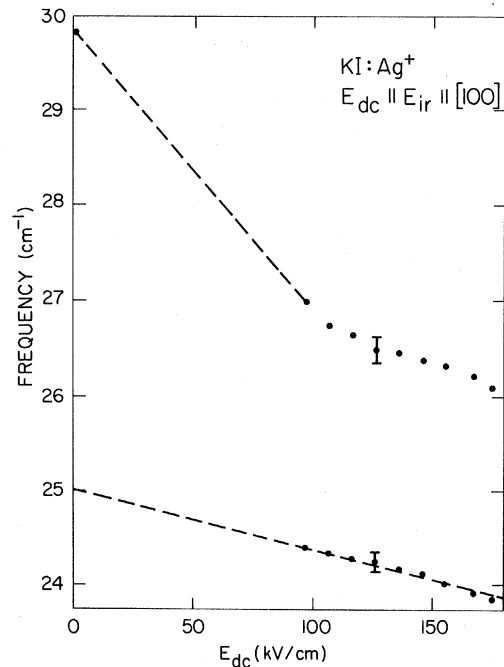

FIG. 5. Frequency vs external electric-field results for the A_{1g} symmetry resonant mode and the 29.8-cm^{-1} line. Here, $E_{ir} \parallel E_{dc} \parallel [100]$. The circles are the experimental data. The curves are explained in the text.
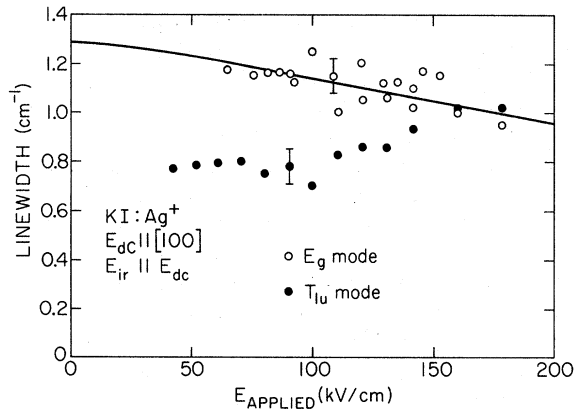
FIG. 6. Linewidth (FWHM absorption) vs external electric-field results for the T_{1u} and E_g symmetry resonances. Here, $E_{ir} \| E_{dc} \| [100]$. No corrections have been made for the instrumental resolution of 0.35 cm^{-1}.

transforming as the A_1 and B_1 irreducible representations of C_{2v}. Both of these levels are optically active, the A_1 for $E_{ir} \| E_{dc}$ and the B_1 for $E_{ir} \| [1\bar{1}0]$ $\perp E_{dc}$. This analysis agrees with the experimental results and confirms that the mode in zero field has E_g symmetry.

Figure 5 shows the experimental-frequency-vs-field points for the 29.8-cm^{-1} line and the field-induced 25-cm^{-1} line for the $E_{ir} \| E_{dc} \| [100]$. No reliable frequencies could be obtained in the low-field region, but the field dependence of the 29.8-cm^{-1} line below ~ 100 kV/cm must be very strong if it is to move up to its zero-field position. This is schematically indicated by the dashed line in Fig. 5. This may mean that the 25-cm^{-1} line also has a strong low-field dependence so that its zero-field frequency is higher than 25-cm^{-1}.

An A_{1g} mode should be observed with $E_{ir} \| E_{dc}$ for both [100] and [110] fields, but not for $E_{ir} \perp E_{dc}$. The Ag$^+$ concentrations in the samples used for the $E_{ir} \| E_{dc} \| [110]$ measurements were apparently too low for either the 25-cm^{-1} line or shifts of the 29.8-cm^{-1} line to be observed. It is more significant that the 25-cm^{-1} line was *not* observed with $E_{dc} \|$ [110] and $E_{ir} \| [1\bar{1}0]$ even though shifts of the 29.8-cm^{-1} line were observed. In view of this, we conclude that the even-parity mode near 25 cm^{-1} does have A_{1g} symmetry in zero field.

The linewidths (FWHM absorption) exhibit some weak field dependences, as shown in Fig. 6 for $E_{ir} \| E_{dc} \| [100]$. The T_{1u}-mode linewidth (closed circles) increases by ~ 25% with increasing field, as does the A_{1g}-mode linewidth (not shown). However, the E_g-mode linewidth (open circles) appears to *decrease* by a few percent with increasing field. The solid curve has been fit to the E_g-mode linewidth and will be explained in Sec. III.

C. Raman Measurements

Some preliminary Raman spectra of KI : Ag$^+$ were obtained using a Spex double monochrometer and a Coherent Radiation Model 52 argon-ion laser operating with ~ 1 W of power at 4880 or 5145 A. Photon-counting techniques were employed to improve the signal-to-noise ratio. The symmetries of any observed scattering peaks could be determined by appropriate combinations of light polarization and crystal orientation. The sample was cooled to 8 K using a commercially available optical cryostat. During the course of a scan, the sample temperature remained constant to better than 1 K.

Figure 7 shows the 5145-A Raman spectrum of a [110]-cut KI : Ag$^+$ sample for a scattering geometry of $z(yx)y$, which yields scattered light from E_g symmetry states. As can be seen, there is a peak at 16.1 ± 0.5 cm^{-1}, in good agreement with the far-infrared results. The linewidth of ~ 3 cm^{-1} is primarily determined by the spectrometer slit width. We were unable to see a Raman peak due to the 25-cm^{-1} A_{1g} mode, most likely because of the much greater Rayleigh scattering which occurs for that particular scattering configuration.

III. FORMULATION OF MODEL

A. Harmonic-Lattice Calculations

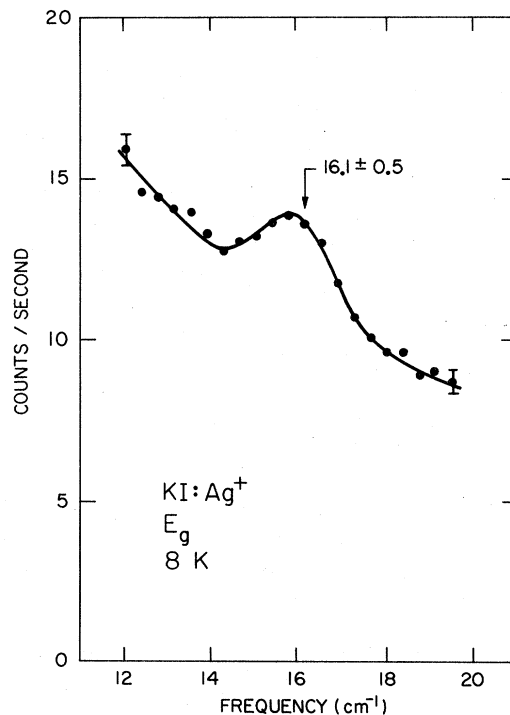To understand the dynamics of the KI : Ag$^+$ defect-

FIG. 7. E_g symmetry Raman-scattering spectrum of KI:Ag$^+$ at 8 K. The scattering geometry is $z(yx)y$, with $x \| [110]$, $y \| [\bar{1}10]$, and $z \| [001]$. The instrumental resolution is 2 cm^{-1}.

A_{1g}

(a)

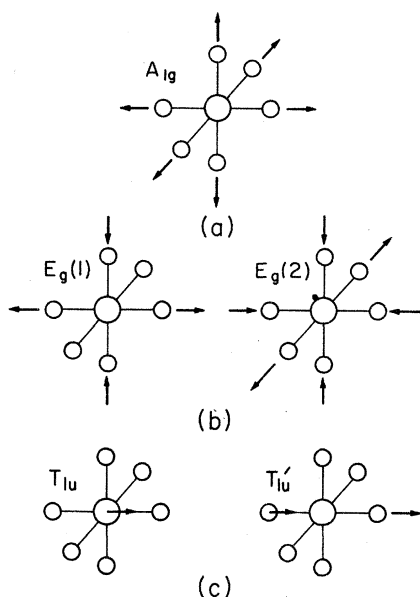$E_g(1)$ $E_g(2)$

(b)

T_{1u} T_{1u}'

(c)

FIG. 8. Normal modes of an XY_6 molecule.

lattice system, we first look to a harmonic near-est-neighbor (nn) model which includes central-force-constant changes, as has been described by Klein.[15] It will be seen that such a simplified model cannot explain the experimental results, but it does offer a physical picture of the possible mo-tional states which can cause the observed far-in-frared and Raman spectra of KI : Ag$^+$. In this model, the central displacements of the impurity and its six nn form a 9×9 reducible representation of the octahedral group O_h. This group representation can be reduced by considering the normal modes of the XY_6 molecule formed by the impurity and its nn. The XY_6 normal modes are found to be an A_{1g} "breathing" mode, as shown in Fig. 8(a); an E_g "tetragonal" mode, both components of which are shown in Fig. 8(b); and two T_{1u} modes, with one component of each shown in Fig. 8(c). The two T_{1u} modes are normally coupled together when the full lattice-dynamical problem is considered. The modes in Fig. 8 are not true normal modes of the defect-lattice system. They must be considered as linear combinations of the perturbed band modes, which cause a line shape that reflects the system-mode density of states for that particular configura-tion. The important point here is that the nn-cou-pling model can lead to two optically active T_{1u} res-onances (presumably the resonant mode at 17.3 cm^{-1} and the 86.2-cm^{-1} gap mode) and two even-parity resonances, as we have observed in KI : Ag$^+$. The addition of noncentral-force-constant changes or the inclusion of a larger defect space only increases the number of possible resonances. Extensions such as these will certainly be necessary, since

Benedek and Nardell[12] have shown that a nn central-force-constant model cannot give both a low-lying T_{1u} resonant mode and a T_{1u} gap mode in KI : Ag$^+$. Furthermore, using their calculated A_{1g} and E_g Green's functions for positive impurities in KI, it is easy to show that the nn effective coupling con-stant reaches zero long before the even-parity res-onances reach such low frequencies, as we have observed.

In addition to the four resonances just discussed, KI : Ag$^+$ shows several other optically active absorp-tion lines which must be explained. The weak and narrow lines at 55.9 and 63.6 cm^{-1} can be correlat-ed with host-crystal density-of-states peaks, after Dolling et al.[28] These peaks have been seen in KI doped with other impurities,[29,30] but they are par-ticularly sharp in the case of KI : Ag$^+$. The third weak line at 51 cm^{-1} is not yet understood, but we note here that it is at an appropriate frequency to be associated with the 17.3-cm^{-1} resonant-mode third harmonic.

It is then the two broad lines at 29.8 and 44.4 cm^{-1} which have yet to be explained and which will be important in the discussion to follow. We will see that these lines are combination bands, corre-sponding to the simultaneous excitation of one T_{1u}-mode quantum and one even-mode quantum. In the harmonic approximation, the combination bands would not be optically active. However, the strong temperature dependence of the T_{1u} mode observed by Alexander, Hughes, and Sievers[31] and the large uniaxial stress shifts of the T_{1u} mode observed by Nolt and Sievers[32] show that the defect system is very anharmonic. The question remains as to the nature of the anharmonicity.

The uniaxial stress shifts of the T_{1u} mode have been interpreted in terms of coupling of the mode to the host-crystal phonons.[32,33] This would seem to be quite a reasonable assumption. However, Alexander et al.[31] pointed out that coupling to the phonons could not simultaneously explain the tem-perature dependence of the T_{1u} mode and the uniaxial-stress shifts. They used the measured-stress cou-pling coefficients to determine the amount of anhar-monic coupling to the phonons, and found that the calculated temperature dependence of the absorp-tion strength was a factor of 100 too small. Further-more, if they assumed that the T_{1u} mode was anhar-monically coupled to a postulated E_g symmetry res-onance, they obtained reasonable agreement for both the temperature dependence and the stress dependence of the T_{1u} mode. We will see in Sec. IV that these intuitive ideas can be at least partially verified using a simple phenomenological model for the defect-lattice system.

At this point, it is worthwhile to discuss another mechanism which may be of importance in the KI : Ag$^+$ system. In the case of the U-center local mode

in alkali halides, it appears that higher-order di-pole moment effects are responsible for a few per-cent of the observed phonon sideband structure.[6,7] Klein[15] has pointed out that second-order dipole-moment terms may be even more important for resonant modes than for local modes. This would seem to be especially true for KI: Ag$^+$, since Ag$^+$ has a tendency to form covalent bonds,[34] and this could be important for the charge-transfer mech-anism which gives rise to a second-order dipole moment.

As shown in the Appendix, a second-order dipole moment can make the combination bands optically active, and also cause an electric-field-induced mixing of the modes. In fact, the field-induced shifts due to a second-order dipole moment are iden-tical in form to the field-induced shifts produced by an anharmonic coupling of the odd- and even-parity modes. Thus, the measurements presented here cannot distinguish between the two mechanisms. However, to explain the uniaxial-stress dependence and the temperature dependence of the T_{1u} mode, we have seen that large anharmonic terms are nec-essary. So we will proceed, in Sec. III B, with a perturbation treatment of the even-odd anharmonic coupling, realizing that higher-order dipole-mo-ment effects may also be important.

B. Anharmonic-Oscillator Model

The observation of two T_{1u} symmetry modes and two even-parity resonances, all of which are quite narrow, makes feasible a phenomenological treat-ment of the resonances and their interactions. As a first approximation then, we assume that the T_{1u}, A_{1g}, and E_g resonances can be treated as indepen-dent harmonic oscillators. No evidence that the gap mode participates in the coupled motion has yet been found, so it will not be considered here. Then, neglecting the phonons, the harmonic Ham-iltonian may be written

$$H_0 = \sum_{i=1}^{3} (P_{Ti}^2 / 2M_T) + \sum_{i=1}^{3} \frac{1}{2} M_T \Omega_T^2 Q_{Ti}^2$$

$$+ \sum_{i=1}^{2} (P_{Ei}^2 / 2M_E) + \sum_{i=1}^{2} \frac{1}{2} M_E \Omega_E^2 Q_{Ei}^2 + P_A^2 / 2M_A$$

$$+ \frac{1}{2} M_A \Omega_A^2 Q_A^2, \quad (2)$$

where the subscripts A, E, and T refer to the A_{1g}, E_g, and T_{1u} modes, respectively, the Q's are the mode normal coordinates, the M's are the oscillator effective masses, and the Ω's are the corresponding resonant frequencies. In the absence of a lattice-dynamical calculation, the oscillator masses are not known since the amplitudes of vibration may be large far away from the impurity site. For sim-plicity, we take $M_T = M(\text{Ag}^+)$, $M_A = M_E = M(\text{I}^-)$, The eigenvectors of H_0 are denoted by $|klm; rs; t\rangle$,

with associated eigenvalues $(k + l + m + \frac{1}{2})\hbar\Omega_T$ $+ (r + s + \frac{1}{2})\hbar\Omega_E + (t + \frac{1}{2})\hbar\Omega_A$, in an obvious notation. In this approximation, infrared-absorption mea-surements would lead to a single (δ-function) line at Ω_T, and Raman scattering would give lines of A_{1g} and E_g symmetries at Ω_A and Ω_E, respectively.

To include the effects of anharmonicity, we ex-pand the potential energy in powers of the harmonic-mode normal coordinates. Because of the inver-sion symmetry about the defect site, the (odd-par-ity) T_{1u}-mode coordinates must enter only as even powers. Then the lowest-order terms in the an-harmonic potential will be of the forms $Q_{Ti}^2 Q_{Ej}$ and $Q_{Ti}^2 Q_A$. Static potential terms such as Q_{Ei}^3 will not be considered, nor will coupling between the two even-parity modes be included. These terms may be important in determining the perturbed even-mode energies, but they cannot be responsible for the presence of the combination bands in the infra-red absorption spectrum. Neither can they lead to a strong electric-field dependence, because of the large oscillator masses.[35,23]

Then using the transformation properties of the system normal modes, the most general form of the cubic interaction between the T_{1u} mode and the even-parity modes may be written

$$H_A^{(3)} = V_A(Q_{T1}^2 + Q_{T2}^2 + Q_{T3}^2) Q_A$$

$$+ V_E[(2Q_{T1}^2 - Q_{T2}^2 - Q_{T3}^2) Q_{E2} + \sqrt{3}(Q_{T2}^2 - Q_{T3}^2) Q_{E1}].$$

$$(3)$$

$H_A^{(3)}$ will enter in second order of perturbation theory. The quartic terms, which are of the form $Q_{Ti}^2 Q_{\text{even}}^2$, will enter in first order, and so are ex-pected to contribute to the perturbed energies in the same order as $H_A^{(3)}$. However, the quartic terms cannot cause the combination bands to be optically active, and they cannot cause a first-order electric-field-induced mixing of the even- and odd-parity modes. Furthermore, a large quartic anharmonicity would cause quadratic com-ponents in the stress-induced frequency shifts of the T_{1u} resonant mode, whereas the experimental shifts are found to be linear.[32] For these reasons, we consider only the perturbation $H_A^{(3)}$ in what fol-lows. The one-dimensional analog of this perturba-tion calculation has been considered by Hughes,[36] in a slightly different context.

We treat $H_A^{(3)}$ as a perturbation, finding the sec-ond-order perturbed energies ϵ_{klm}^{rst}, and the first-order perturbed eigenvectors $|\psi_{klm}^{rst}\rangle$. The per-turbed transition energies from the ground state are listed in Table II for some of the lower-energy states.

IV. COMPARISON WITH EXPERIMENT

A. Zero-Field Absorption Spectrum

One method of proceeding now would be to fit the

TABLE II. Perturbed transition energies from the anharmonic-oscillator model, where $U_E = V_E/8M_T\Omega_T \times (\hbar/2M_E\Omega_E)^{1/2}$ and $U_A = V_A/4M_T\Omega_T (\hbar/2M_A\Omega_A)^{1/2}$.

Final state	Perturbed transition energy
$\lvert 100; 00; 0 \rangle$	$\hbar\Omega_T - \dfrac{4U_E^2}{\Omega_E} - \dfrac{4U_E^2}{2\Omega_T+\Omega_E} - \dfrac{8U_A^2}{\Omega_A} - \dfrac{2U_A^2}{2\Omega_T+\Omega_A}$
$\lvert 000; 10; 0 \rangle$	$\hbar\Omega_E - \dfrac{3U_E^2}{2\Omega_T-\Omega_E} - \dfrac{3U_E^2}{2\Omega_T+\Omega_E}$
$\lvert 000; 00; 1 \rangle$	$\hbar\Omega_A - \dfrac{3U_A^2}{2\Omega_T-\Omega_A} - \dfrac{3U_A^2}{2\Omega_T+\Omega_A}$
$\lvert 100; 10; 0 \rangle$	$\hbar\Omega_T + \hbar\Omega_A - \dfrac{4U_E^2}{\Omega_E} - \dfrac{4U_E^2}{2\Omega_T+\Omega_E} - \dfrac{8U_A^2}{\Omega_A}$
	$\qquad - \dfrac{5U_A^2}{2\Omega_T-\Omega_A} - \dfrac{7U_A^2}{2\Omega_T+\Omega_A}$
$\lvert 100; 00; 1 \rangle$	$\hbar\Omega_T + \hbar\Omega_E - \dfrac{4U_E^2}{\Omega_E} - \dfrac{11U_E^2}{2\Omega_T+\Omega_E} - \dfrac{7U_E^2}{2\Omega_T-\Omega_E}$
	$\qquad - \dfrac{8U_A^2}{\Omega_A} - \dfrac{2U_A^2}{2\Omega_T+\Omega_A}$

perturbed energies of Table II to the observed mode frequencies and so obtain values for the anharmonicity coefficients V_A and V_E of Eq. (3). This can be done analytically, but it is not very meaningful since many anharmonic terms which may contribute to the mode shifts in the same order as $H_A^{(3)}$ have been neglected. In fact, if this calculation is done, we find that V_A must be imaginary. While an imaginary coupling coefficient is not necessarily devoid of physical meaning, it most likely indicates that the neglected anharmonic terms are important. We then conclude that it is more reasonable to determine V_A and V_E from the strengths of the combination bands for, as pointed out earlier, these quantities are nearly independent of the cubic and quartic terms not included in the perturbation calculation.

For this purpose, we must calculate the electric dipole matrix elements connecting the perturbed ground state $\lvert \psi_{000}^{000} \rangle$ with the T_{1u} components of the $E_g + T_{1u}$ and $A_{1g} + T_{1u}$ combination bands. The $E_g + T_{1u}$ band consists of two three-fold degenerate states, transforming as $E_g \times T_{1u} = T_{2u}$. The T_{1u} level will be optically active, and we find the ratio of its integrated absorption strength to that of the T_{1u} resonant mode to be

$$S(E_g + T_{1u})/S(T_{1u}) = 8\hbar_E^2(\Omega_T + \Omega_E)/$$

$$M_T^2 M_E \Omega_T \Omega_E^3 (2\Omega_T + \Omega_E)^2. \qquad (4)$$

The $A_{1g} + T_{1u}$ combination band consists only of one T_{1u} level, and we calculate a similar ratio

$$S(A_{1g} + T_{1u})/S(T_{1u}) = 2\hbar V_A^2(\Omega_T + \Omega_A)/$$

$$M_T^2 M_A \Omega_T \Omega_A^3 (2\Omega_T + \Omega_A)^2. \qquad (5)$$

In calculating these expressions, it is assumed that the perturbed-mode frequencies can be approximated by the harmonic-mode frequencies. Using the values of the ratios given in Table I, setting $M_A = M_E = M(\text{I}^-)$, $M_T = M(\text{Ag}^+)$, and assuming that the harmonic frequencies can be replaced by the observed frequencies, we calculate $V_E = 5.7 \times 10^{11}$ and $V_A = 1.8 \times 10^{12}$ erg/cm^3. These coefficients are very large, so that the system is very anharmonic. From the expressions for the perturbed energies of Table II, we calculate that coupling coefficients this large lead to anharmonic shifts of the T_{1u} resonant frequency of ~ 10 cm^{-1}, so that the anharmonic contributions to the oscillator energies are nearly as large as the harmonic contributions. This means that a perturbation calculation cannot be expected to be quantitatively correct. It can, however, give a semiquantitative indication of the importance of the anharmonic coupling, as we now show.

B. Electric-Field Dependence of the Absorption Spectrum

The electric-field-dependence results can verify the form of the coupling terms used in the perturbation calculation. The application of an external electric field in the [100] direction introduces the perturbation

$$H_E = - e_0^* E_i Q_{T1}, \qquad (6)$$

where E_i is the local electric field at the impurity site, and e_0^* is the effective charge associated with the odd-parity mode. Since the E_g and T_{1u} (perturbed) modes are nearly degenerate, we let 2Δ be their zero-field separation and do first-order degenerate perturbation theory with H_E. This leads to a mixing of the two modes and results in the field-induced shifts (for $E_{1r} \parallel E_{dc}$)

$$W(E_i) = \pm (\Delta^2 + R^2 E_i^2)^{1/2}, \qquad (7)$$

where

$$R = 2e_0^*\hbar V_E/(2\Omega_T - \Omega_E)\Omega_E M_T(M_T M_E \Omega_T \Omega_E)^{1/2}.$$

The plus and minus signs in Eq. (7) are to be associated with the T_{1u} and E_g modes, respectively. The results of extending this calculation to the other field and polarization directions are summarized in Table III.

The solid curves in Fig. 4 show the calculated shifts of Table III. The value of R (and hence of V_E) has been chosen to fit the [100]-field dependence of the E_g mode. The agreement for the other E_g-component shifts is quite satisfactory, and so offers evidence that cubic anharmonicity is the dominant mixing mechanism involved. The value $V_E = 3.7 \times 10^{11}$ erg/cm^3 (setting $e_0^* = \lvert e \rvert$ and making the Lorentz local-field correction) calculated from the fit to the experimental curves compares favorably with the estimate of V_E obtained from the strength

TABLE III. Calculated electric-field shifts of the E_g- and T_{1u}-mode components, where $R = 2e_0^* \hbar V_E/(2\Omega_T - \Omega_E) \times \Omega_E M_T (M_T M_E \Omega_T \Omega_E)^{1/2}$.

Polarization		Calculated shifts
E_{dc}	E_{ir}	
[100]	[100]	$\pm (\Delta^2 + R^2 E_i^2)^{1/2}$
[100]	[001]	0
[110]	[110]	$\pm (\Delta^2 + \frac{1}{4} R^2 E_i^2)^{1/2}$
[110]	[1$\bar{1}$0]	$\pm (\Delta^2 + \frac{3}{4} R^2 E_i^2)^{1/2}$
[110]	[001]	0

of the $E_g + T_{1u}$ combination band.

In Fig. 4, the experimental shifts of the T_{1u}-mode components are all smaller than the calculated values. This indicates that mixing of the A_{1g} and T_{1u} modes should also be considered. The T_{1u}-mode shifts resulting from the $A_{1g} - T_{1u}$ mixing are easily estimated to be on the order of 1 cm^{-1} for $E_{dc} = 200$ kV/cm. There must however be other contributing factors, such as coupling to the host-crystal phonons, since the E_g- and T_{1u}-mode components do not shift equal amounts when $E_{dc} \parallel [110]$ and E_{ir} $\parallel [1\bar{1}0]$. In this particular field configuration, the $A_{1g} - T_{1u}$ mixing cannot cause any shifts.

The field dependences of the A_{1g} resonances and the 29.8-cm^{-1} combination band are more difficult to understand. We consider Fig. 9, which shows a schematic diagram of the perturbed energy levels. Those levels indicated by a solid line have been observed experimentally. Those denoted by dashed lines have not been observed, but are predicted by the anharmonic-oscillator model. The T_{1u}- and E_g-mode second harmonics in the 30–35-cm^{-1} region are quite likely responsible for the "anomalous" electric-field shifts of the 29.8-cm^{-1} combination band. The combination band is predicted to be strongly mixed by the electric field with the mode second harmonics, and only weakly mixed with the 25-cm^{-1} A_{1g} resonance, resulting in a net downward shift. However, the weak mixing between the A_{1g} even mode and the combination band creates some difficulties of its own. An estimate shows that the A_{1g} mode should be shifted slightly *up* in frequency by an electric field, since the mixing with the 17.3-cm^{-1} T_{1u} mode is stronger than that with the 29.8-cm^{-1} combination band.

Broadening of the absorption lines with field is due to at least two contributions. Nonuniform field broadening would be expected to cause an additional linewidth proportional to the magnitude of the frequency shift of the line. Another source of broadening is due to the changing phonon density of states as the line is shifted up or down in frequency. Since the density of states is proportional to ω^2, this con-

tribution to the linewidth should also vary as ω^2. The solid curve in Fig. 6 is a least-squares fit to these two broadening terms of the form

$$\Gamma = \alpha [\Omega_E (E_i) - \Omega_E (0)] + \beta \Omega_E^2 (E_i). \tag{8}$$

The coefficient β is found to be $\beta = 0.0048$ cm. While the data points do show a good deal of scatter, the fit of the curve is evidence that the linewidth of the E_g resonance is primarily determined by one-phonon decay.

C. Uniaxial-Stress Results

The KI: Ag$^+$ T_{1u} resonance at 17.3 cm^{-1} is known to undergo large frequency shifts with an applied uniaxial stress.[32] We will show here that large stress-induced shifts are consistent with the anharmonic-oscillator model. Using the cluster model described by Alexander et al.,[31] in which only coupling of the defect to its nn is assumed to be important, it can be shown that

$$V_A = \sqrt{3} \, AM_T \Omega_T / \sqrt{2} \hbar a, \quad V_E = \sqrt{3} \, BM_T \, \Omega_T / \hbar a,$$

where A and B are the A_{1g} and E_g stress coupling
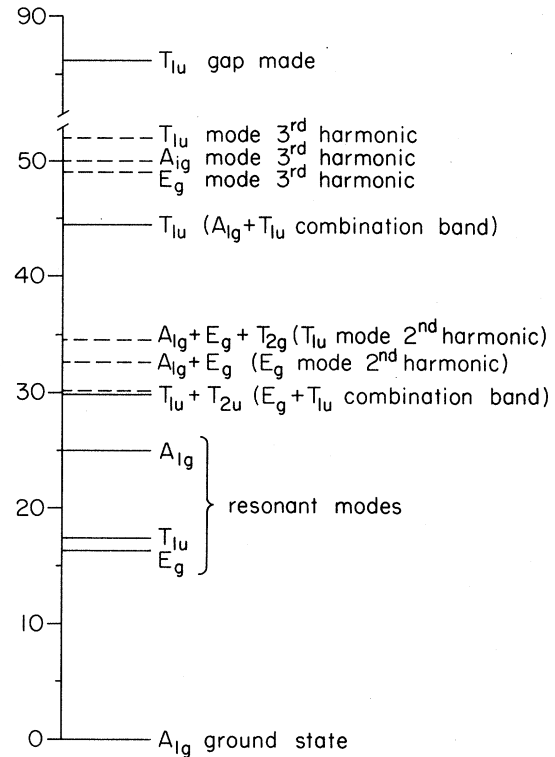

FIG. 9. Schematic diagram of the perturbed vibrational energy levels of KI:Ag$^+$. Those levels indicated by a solid line have been observed experimentally. Those denoted by a dashed line have not been observed, but are predicted by the anharmonic-oscillator model. Mode harmonics higher than the third are not included in this figure.

coefficients,[32] respectively, and a is the nn distance. Using the measured values of A and B, corrected for the local compliances at the impurity site,[37] we calculate $V_E = 8.8 \times 10^{11}$ and $V_A = 1.36 \times 10^{12}$ erg/cm^3. These values are only in rough agreement with our earlier estimates. This is not too surprising considering the many approximations which have been made. Furthermore, the values of V_A and V_E obtained from the strengths of the combination bands are a measure of the *dynamic* coupling of the T_{1u} mode to the two even modes. The stress measurements on the other hand probe the static coupling. There is no *a priori* reason why these two coupling coefficients should be the same. Perhaps more important is the fact that the local compliances used in determining the stress coupling coefficients were calculated from a nn central-force-constant model,[33] which is clearly not adequate for KI : Ag$^+$. The important feature here is that the anharmonic-oscillator model can give rise to stress shifts of magnitude similar to those observed.

D. Temperature of T_{1u} Mode

One of the more striking features of the T_{1u} symmetry resonant modes in alkali halides is their rapid temperature dependence. This is particularly true of KI : Ag$^+$, where it has been found that the integrated absorption strength of the T_{1u} mode decreases by a factor of 5 by 15 K. Alexander, Hughes, and Sievers[31] (hereafter referred to an AHS) showed that this aspect of the temperature dependence could not be explained in terms of linear coupling of the resonant mode to a Debye spectrum of phonons, but some measure of agreement with experiment could be obtained if linear coupling of the T_{1u} mode to a postulated even-parity resonance of E_g symmetry was included. We treat these ideas here using the perturbation approach outlined earlier.

In contrast to linear-coupling theory, as applied by AHS, the perturbation approach does not give a simple analytic solution for the temperature dependence. Here, even a three-dimensional calculation is rather formidable, and to make the problem somewhat more tractable, we resort to a one-dimensional calculation in which the A_{1g}, E_g, and T_{1u} modes are treated as if they were singly degenerate. Then the transition energy from a perturbed initial state $|n_T n_E n_A\rangle$ to a final state $|n_T + 1; n_E n_A\rangle$ is given by

$$\Delta\Omega(n_T, n_E, n_A) = \Omega_T - \sum_{i=A,E} \frac{V_i^2 \hbar^2}{4 M_T^2 \Omega_T^2 M_i \Omega_i}$$
$$\times \left[\frac{4(n_T + 1)}{\Omega_1} + \frac{n_T + 2n_i + 2}{2\Omega_T + \Omega_i} + \frac{2n_i - n_T}{2\Omega_T - \Omega_i} \right]. \quad (9)$$

The integrated absorption strength of the T_{1u}

mode is then given by

$$\int_{T_{1u}\text{ mode}} \alpha(\nu) d\nu$$

$$= \sum_{n_T, n_E, n_A} \{ (4\pi^2/3c\hbar n) \Delta\Omega(n_T, n_E, n_A)[P(n_T, n_E, n_A) $$
$$- P(n_T + 1, n_E, n_A)] |\mu(n_T, n_E, n_A)|^2 \}, \quad (10)$$

where $P(n_T, n_E, n_A)$ is the Boltzmann population of the state $|n_T n_E n_A\rangle$, and $\mu(n_T, n_E, n_A)$ is the electric dipole matrix element connecting $|n_T n_E n_A\rangle$ with $|n_T + 1; n_E n_A\rangle$. To obtain $\mu(n_T, n_E, n_A)$, the wave functions must be calculated to second order. We have evaluated Eq. (10) by a computer calculation, including all states up to $n_T = n_E = n_A = 4$. For temperatures below 15 K, the error incurred in neglecting higher energy states should be negligible. Using the values of the anharmonic coupling coefficients determined from the strengths of the combination bands, the calculation predicts that the integrated absorption strength of the T_{1u} mode at 15 K should be 66% of the low-temperature strength. This should be compared with the experimental results of AHS, who found that the 15-K strength is 20% of the low-temperature strength.

E. Thermal Conductivity

Baumann and Pohl[17] have measured the low-temperature thermal conductivity of KI : Ag$^+$, finding a dip at 4 K, which indicates the presence of a resonance at 12 cm^{-1} ± 20%. This estimated frequency is somewhat lower than either the E_g or T_{1u} resonances. The 25-cm^{-1} A_{1g} resonance would be expected to cause a thermal conductivity dip near 8 K.[17] Experimentally, the E_g-mode linewidth is found to be a factor of 3 larger than the T_{1u}-mode linewidth. (In making this comparison, it is necessary to use a T_{1u}-mode linewidth of 0.4 cm^{-1}, as has been measured for isotopically pure Ag$^+$ impurities.[13] The presence of both ^{107}Ag$^+$ and ^{109}Ag$^+$ isotopes increases the measured T_{1u}-mode linewidth to 0.6 cm^{-1}, but is expected to have little effect on the even-mode linewidths.) The E_g-mode linewidth also appears to show the frequency dependence expected for a resonance coupled to the phonons. The greater linewidth of the E_g resonance might suggest that it is the more important of the two in determining the low-temperature thermal conductivity. Klein[38] has recently calculated that the phonon scattering by a resonant mode obeys a "peak-scattering theorem," which says that all resonances of the same degeneracy and frequency in a given host lattice should have the same peak-mean-scattering rate, independent of their widths or shapes. The total scattering strength however varies as (linewidth)^2. Since the frequencies of the two modes are not very different, one would on this basis ex-

pect the E_g mode to be ~ 6 times as effective as the T_{1u} mode in producing a low-temperature thermal conductivity dip. A possible experimental test of this result is to measure the thermal conductivity of KI : Ag$^+$ with an electric field applied. However, the analyses of such results would be complicated by the nearly complete mixing of the E_g and T_{1u} modes in the high-field region.

V. SUMMARY AND CONCLUSIONS

KI: Ag$^+$ shows a complex far-infrared absorption spectrum, with seven optically active energy levels below the TO phonon frequency. We have observed resonant modes of A_{1g}, E_g, and T_{1u} symmetries, as well as a T_{1u} symmetry gap mode. The presence of four resonant modes with these symmetries is predicted by a nn central-force-constant change model, but the observed resonant frequencies are not consistent with a single force-constant change. Part of the reason for this may be that the system is very anharmonic, but a more plausible explanation is that the defect space used in the lattice-dynamical calculations[12] was too small. The low frequencies of the even-parity resonance strongly suggest that the lattice-relaxation model of Gethins et al.,[16] which includes force-constant changes between the impurity's nearest neighbors and its fourth nearest neighbors along [100], would be more realistic.

The presence of the $A_{1g} + T_{1u}$ and $E_g + T_{1u}$ combination bands and the strong electric-field-induced mixing of the odd- and even-parity resonant modes demonstrates that the two types of resonance are strongly coupled. We have found some agreement between the experimental results on KI: Ag$^+$ and a model in which the T_{1u} symmetry resonant mode is anharmonically coupled to the observed A_{1g} and E_g symmetry resonances. The perturbation treatment given here explains semiquantitatively the presence of the combination bands and the electric-field shifts of the modes, as well as the uniaxial-stress dependence of the T_{1u} mode. The agreement for the temperature dependence of the T_{1u} mode is less satisfactory, but this may be expected in view of the many simplifications used in the calculation.

The question arises as to whether the lack of good agreement for all of the experimental results stems only from the use of an oversimplified model, or if, in addition, there are other mechanisms which are important and have not been taken into account. One purpose of this section is to discuss this aspect of the problem.

The model calculation suffers from several drawbacks. First, the perturbation is rather large. The values of the anharmonic coupling coefficients suggest that the T_{1u} mode is shifted by ~ 10 cm^{-1} by the anharmonicity. Such a large anharmonic contribution to the energy is hardly con-

sistent with a perturbation treatment, so that good quantitative agreement cannot be expected.

Second, we have neglected any quartic anharmonicity and any static anharmonicity. Simple arguments tell us that quartic anharmonicity (taken to first order) should be as important as cubic anharmonicity (taken to second order) in determining the perturbed mode energies. Yet, this appears to be inconsistent with a linear shift of the T_{1u}-mode frequency under uniaxial stress.

Third, no coupling of the resonance to the host-crystal phonons has been included. Such coupling can clearly lead to additional anharmonic shifts of the modes, cause large uniaxial-stress shifts, and explain some features of the temperature dependence.[39] However, it cannot produce the large observed electric-field shifts or the combination bands, and it cannot explain the temperature dependence of the strength of the T_{1u} mode.

The combination bands and the electric-field shifts of the modes can be explained by cubic anharmonicity, but these results are equally consistent with the presence of a second-order dipole moment. A second-order dipole moment by itself, however, cannot cause the observed uniaxial-stress shifts and temperature dependence of the T_{1u} mode. It has been shown[40] that these two mechanisms are not independent, and furthermore that a large second-order dipole moment implies a large cubic anharmonicity. Thus it appears that both effects will have to be included consistently if we are to understand the KI: Ag$^+$ vibrational spectrum.

While we have not been able to obtain good quantitative agreement with all of the experimental results of KI : Ag$^+$, the inadequacy of the nn central-force-constant change model and the importance of anharmonicity for KI : Ag$^+$ have been demonstrated.

APPENDIX: SECOND-ORDER DIPOLE MOMENT EFFECTS

To include a second-order dipole moment, we start with the harmonic oscillator Hamiltonian [Eq. (2)] and expand the dipole moment $\vec{M}$ in terms of the resonant-mode normal coordinates. If we consider only central motion of the impurity and its neighbors, we may write

$$\vec{M} = \sum_{i=1}^{3} e_0^* \vec{Q}_{Ti} + \sum_{i,j=1}^{3} a_{ij} Q_i^{even} \vec{Q}_{Tj} = \vec{M}^{(1)} + \vec{M}^{(2)},$$

$$(A1)$$

where Q_i^{even} is one of the even-mode coordinates Q_{E1}, Q_{E2}, or Q_A, $\vec{M}^{(1)}$ is the linear dipole moment, and $\vec{M}^{(2)}$ is the second-order dipole moment.

Using group-theoretical arguments, it is easily shown that there are only two independent coefficients a_{ij}, so that the x, y, and z components of the second-order dipole moment may be written

$$M_x^{(2)} = 2S_E Q_{E2}Q_{T1} + S_A Q_A Q_{T1} ,$$

$$M_y^{(2)} = -S_E Q_{E2}Q_{T2} + \sqrt{3} S_E Q_{E1}Q_{T2} + S_A Q_A Q_{T2} , \quad \text{(A2)}$$

$$M_z^{(2)} = -S_E Q_{E2}Q_{T3} - \sqrt{3} S_E Q_{E1}Q_{T3} + S_A Q_A Q_{T3} ,$$

where S_A and S_E are constants, and Q_{E1} and Q_{E2} are the E_g-mode normal coordinates, as shown in Fig. 8(b).

The first point to notice is that a second-order dipole moment will make the even-odd combination bands optically active. The ratios of the integrated absorption strengths of the $A_{1g} + T_{1u}$ and $E_g + T_{1u}$ combination bands to that of the T_{1u} resonant mode are found to be

$$S(A_{1g} + T_{1u})/S(T_{1u}) = \hbar S_A^2 (\Omega_T + \Omega_A)/2e_0^{*2} M_A \Omega_A \Omega_T ,$$

$$\text{(A3)}$$

$$S(E_g + T_{1u})/S(T_{1u}) = 2\hbar S_A^2(\Omega_T + \Omega_E)/e_0^{*2} M_E \Omega_E \Omega_T .$$

Assuming that the observed combination bands are due *only* to a second-order dipole moment, we calculate $S_A = 0.2$ and $S_E = 0.1$ statC/cm, using the absorption strengths of Table I. These values for the second-order dipole-moment coefficients are an order of magnitude larger than those estimated for pure KI by Xinh.[7]

A second-order dipole moment also leads to electric-field-induced mixing of the T_{1u} resonance with the even-parity resonances. For simplicity,

and to facilitate comparison with the cubic anharmonicity calculation, we include here only mixing of the T_{1u} and E_g modes.

Applying a local electric field $\vec{E}_l$ in the [100] (x) direction reduces the site symmetry from O_h to C_{4v} and introduces the perturbation

$$H_S = -\vec{M}^{(2)} \cdot \vec{E}_l = -M_x^{(2)} E_l = -2S_E Q_{E2}Q_{T1}E_l . \quad \text{(A4)}$$

From first-order degenerate perturbation theory with H_S, we then obtain secular equation

$$
\begin{array}{c}
\begin{array}{ccccc}
T_{1u}(x) & T_{1u}(y) & T_{1u}(z) & E_g(1) & E_g(2)
\end{array} \\
\begin{array}{c}
T_{1u}(x) \\
T_{1u}(y) \\
T_{1u}(z) \\
E_g(1) \\
E_g(1)
\end{array}
\begin{bmatrix}
\Delta - W & 0 & 0 & \epsilon E_l & 0 \\
0 & \Delta - W & 0 & 0 & 0 \\
0 & 0 & \Delta - W & 0 & 0 \\
\epsilon E_l & 0 & 0 & -\Delta - W & 0 \\
0 & 0 & 0 & 0 & -\Delta - W
\end{bmatrix} = 0 ,
\end{array}
$$

$$\text{(A5)}$$

where 2Δ is the $E_g - T_{1u}$ zero-field splitting, and

$$\epsilon = -\hbar S_E/(M_T \Omega_T M_E \Omega_E)^{1/2} .$$

Equation (A5) has the solutions

$$W(A_1) = \pm (\Delta^2 + \epsilon^2 E_l^2)^{1/2} ,$$

$$W(B_1) = -\Delta , \qquad W(E) = +\Delta , \quad \text{(A6)}$$

where A_1, B_1, and E are irreducible representations of the C_{4v} point group.

With a [110] field applied, the site symmetry becomes C_{2v}, and the perturbation is

$$H_S = -2S_E E_l Q_{E2}Q_{T1} + (\tfrac{1}{2} S_E E) Q_{E2}Q_{T2}$$

$$-\tfrac{1}{2} \sqrt{3} S_E E_l Q_{E1}Q_{T2} , \quad \text{(A7)}$$

which leads to the secular equation

$$
\begin{bmatrix}
\Delta - W & 0 & 0 & \epsilon E_l/\sqrt{2} & 0 \\
0 & \Delta - W & 0 & -\epsilon E_l/2\sqrt{2} & \sqrt{3}\,\epsilon E_l/2\sqrt{2} \\
0 & 0 & \Delta - W & 0 & 0 \\
\epsilon E_l/\sqrt{2} & -\epsilon E_l/2\sqrt{2} & 0 & -\Delta - W & 0 \\
0 & \sqrt{3}\,\epsilon E_l/2\sqrt{2} & 0 & 0 & -\Delta - W
\end{bmatrix} = 0. \quad \text{(A8)}
$$

This has the solutions

$$W(A_1) = \pm (\Delta^2 + \tfrac{1}{4}\epsilon^2 E_l^2)^{1/2} ,$$

$$W(B_1) = \pm (\Delta^2 + \tfrac{3}{4}\epsilon^2 E_l^2)^{1/2} , \qquad W(B_2) = +\Delta ,$$

where A_1, B_1, and B_2 are irreducible representations of C_{2v}. Assuming that the observed electric-

field-induced shifts of the E_g mode arise *only* because of a second-order dipole moment, we obtain $S_E = 0.15$ statC/cm. This is about the same as our estimate of S_E from the strength of the combination band.

In view of these results, it must be concluded that one cannot distinguish cubic anharmonicity

from second-order dipole effects on the basis of electric-field-induced shifts. The relative shifts of the T_{1u} and E_g components are identical for the two mechanisms.

[1]G. Schaefer, Phys. Chem. Solids 12, 233 (1960).

[2]B. Fritz, U. Gross, and D. Bauerle, Phys. Status Solidi 11, 231 (1965).

[3]T. Timusk and M. V. Klein, Phys. Rev. 141, 664 (1966).

[4]S. S. Jaswal and D. J. Montgomery, Phys. Rev. 138, A1257 (1964).

[5]R. Fieschi, G. F. Nardelli, and N. Terzi, Phys. Rev. 138, A203 (1965).

[6]John B. Page, Jr., and B. G. Dick, Phys. Rev. 163, 910 (1967).

[7]Nguyen X. Xinh, Phys. Rev. 163, 896 (1967).

[8]A. J. Sievers, A. A. Maradudin, and S. S. Jaswal, Phys. Rev. 138, A272 (1965).

[9]I. G. Nolt, R. A. Westwig, R. W. Alexander, Jr., and A. J. Sievers, Phys. Rev. 157, 730 (1967).

[10]A. J. Sievers, Phys. Rev. Letters 13, 310 (1964).

[11]R. Weber, Phys. Letters 12, 311 (1964).

[12]Giorgio Benedek and G. F. Nardelli, J. Chem. Phys. 48, 5242 (1967).

[13]R. D. Kirby, I. G. Nolt, R. W. Alexander, Jr., and A. J. Sievers, Phys. Rev. 168, 1057 (1968).

[14]H. F. Macdonald, M. V. Klein, and T. P. Martin, Phys. Rev. 177, 1292 (1969).

[15]For a comprehensive review of the work on impurities in alkali halides through 1967, see the article by M. V. Klein, in Physics of Color Centers, edited by W. B. Fowler (Academic, New York, 1968), Chap. 7.

[16]T. Gethins, T. Timusk, and E. J. Woll, Phys. Rev. 157, 744 (1967).

[17]F. C. Baumann and R. O. Pohl, Phys. Rev. 163, 843 (1967).

[18]F. C. Baumann, J. P. Harrison, R. O. Pohl, and D. W. Seward, Phys. Rev. 159, 691 (1967).

[19]R. F. Caldwell and M. V. Klein, Phys. Rev. 158, 861 (1967).

[20]R. D. Kirby, Phys. Rev. Letters 26, 512 (1971).

[21]I. G. Nolt, R. D. Kirby, C. D. Lytle, and A. J. Sievers, Appl. Opt. 8, 309 (1969).

[22]H. D. Drew and A. J. Sievers, Appl. Opt. 8, 2067 (1969).

[23]B. P. Clayman, R. D. Kirby, and A. J. Sievers, Phys. Rev. B 3, 1351 (1971).

[24]R. D. Kirby, A. E. Hughes, and A. J. Sievers, Phys. Rev. B 2, 481 (1970).

[25]B. P. Clayman, I. G. Nolt, and A. J. Sievers, Solid State Commun. 7, 7 (1969).

[26]K. F. Renk, Phys. Letters 20, 137 (1966).

[27]C. R. Becker, Solid State Commun. 8, 337 (1970).

[28]G. Dolling, R. A. Cowley, C. Schittenhelm, and I. M. Thorson, Phys. Rev. 147, 577 (1966).

[29]A. J. Sievers and C. D. Lytle, Phys. Letters 14, 271 (1965).

[30]K. F. Renk, Phys. Letters 14, 281 (1965).

[31]R. W. Alexander, Jr., A. E. Hughes, and A. J. Sievers, Phys. Rev. B 1, 1563 (1970).

[32]I. G. Nolt and A. J. Sievers, Phys. Rev. 174, 1004 (1968).

[33]G. Benedek and G. F. Nardelli, Phys. Rev. 167, 837 (1968).

[34]James C. Phillips, in Covalent Bonding in Crystals, Molecules, and Polymers (Chicago U. P., Chicago, 1969).

[35]B. P. Clayman and A. J. Sievers, Phys. Rev. Letters 21, 1453 (1968).

[36]A. E. Hughes, Phys. Rev. 173, 860 (1968).

[37]R. J. Elliott, J. A. Krumhansl, and R. H. Merrett, in Localized Excitations in Solids, edited by R. F. Wallis (Plenum, New York, 1968), p. 709.

[38]Miles V. Klein, Phys. Rev. 186, 839 (1969).

[39]K. H. Timmesfeld, Phys. Status Solidi 30, 73 (1968).

[40]B. Szigeti, Proc. Roy. Soc. (London) 252, 217 (1959).